Fast Design of Jerusalem-Cross Parameters by Equivalent Circuit Model and Least-Square Curve Fitting Technique

Hsing-Yi Chen, Tsung-Han Lin, and Pei-Kuen Li

Department of Communications Engineering
Yuan Ze University, Chung-Li, Taoyuan, 32003, Taiwan
eehychen@saturn.yzu.edu.tw, s1014846@mail.yzu.edu.tw, s1004835@mail.yzu.edu.tw

Abstract **─** Based on an equivalent circuit model, the least-square curve fitting technique is proposed to quickly design optimum values of geometrical parameters of a dual-band Jerusalem-cross element for arbitrarily specifying any dual resonant frequencies. The validity of the least-square curve fitting technique is checked by comparing geometrical parameters and dual resonant frequencies of six Jerusalem-cross grids obtained by the proposed technique with those obtained by the improved empirical model and measurement method. Design of dual-band Jerusalem-cross slots is also conducted by the proposed technique. Simulation results of reflection and dual resonant frequencies of Jerusalem-cross slots designed by the proposed technique are also validated by measurement data.

Index Terms **─** Dual-band Jerusalem-cross element, least-square curve fitting, reflection, transmission.

I. INTRODUCTION

Frequency selective surface (FSS) has been extensively studied for many decades [1-32]. It has many applications in polarizers [1], antenna designs [2-10], transmission improvement for signals through energy-saving glass [11-14], artificial magnetic conductor (AMC) designs [15-17], spatial microwave and optical filters [18-25], absorbers [26-31], and planar metamaterials [32]. The FSS is usually formed by periodic arrays of metallic patches or slots of arbitrary geometries. A FSS with periodic arrays of metallic patches or slots exhibits total reflection or total transmission in the neighborhood of the geometric resonant frequency, respectively. Typical FSS geometries are designed by dipoles, rings, square loops, fractal shapes, etc. Most of these FSSs are used to deal with reflection and transmission problems at a single resonant frequency. It is rather difficult to design FSS elements that offer dual-band responses.

Several numerical methods have been used to design FSS parameters such as method of moments (MoM) [18], finite-difference time-domain (FDTD) method [33-35], and finite-element method (FEM) [36]. These methods have a tedious computation procedure which involves many electromagnetic equations governing FSS theory. In recent years, many electromagnetic simulation commercial software packages are available for the design of FSS parameters, such as Ansoft's HFSS, Ansoft's Designer, and CST Microwave Studio. These commercial software packages are easily used to design FSS parameters. However, the design process of a FSS element using the commercial software package can be divided into preliminary and fine tune steps. In the preliminary design steps, various critical geometrical dimensions of a FSS element are well investigated through parametric study using a full-wave model simulation. Based on preliminary study, the final design can be achieved through fine tuning the critical geometrical parameters to obtain the desired resonant frequencies. This is a non-efficient and labor intensive process due to trial-and-error tests and heavy computational works. Alternatively, the equivalent circuit method [37-39] is much simpler than numerical methods for the design of FSS parameters. In this method, the segments of the FSS structure are modeled as capacitive and inductive components in a transmission line [37-38]. Limitation of the equivalent circuit method is that it can be used only for normal incidence and without substrates.

In this paper, we propose the least-square curve fitting technique [40] to quickly obtain optimum values of geometrical parameters of a dual-band Jerusalem-cross element for arbitrarily specifying any dual resonant frequencies. In the design process, an equivalent circuit model of the frequency characteristic for normal wave incidence [38] is introduced to facilitate the optimum design of a Jerusalem-cross element. In simulations, the transmission and reflection of Jerusalem-cross elements are obtained by using the Ansoft high-frequency structure simulator (HFSS, Ansoft, Pittsburgh, PA). Simulation results of geometrical parameters and dual resonant frequencies of Jerusalem-cross grids obtained by the proposed technique are compared with those

Submitted On: September 20, 2013
Accepted On: May 25, 2015

obtained by the improved empirical model and measurement method presented in the literature [38]. Dual-band Jerusalem-cross slots designed by the proposed technique are also presented. Simulation results of reflection and dual resonant frequencies of Jerusalem-cross slots are validated by measurement data.

II. EQUIVALENT CIRCUIT MODEL OF JERUSALEM-CROSS GRIDS

The equivalent circuit model of Jerusalem-cross grids is a very useful technique to quickly predict the resonant frequencies of their structures. Figure 1 shows a FSS element constructed with Jerusalem-cross grids and its geometrical parameters p, w, s, h, and d. Where p is the periodicity of a unit cell, w is the width of the conductive strip, s is the separation distance between adjacent units, h is the width of the end caps of the Jerusalem-cross, and d is the length of the end caps of the Jerusalem-cross. Based on Langley and Drinkwater's studies [38], for any array of thin, continuous, infinitely long, perfectly conducting Jerusalem-cross FSS for normal incidence EM waves, the equivalent circuit model can be presented as shown in Fig. 2. The series resonant circuit L_1C_1 is used to generate the lower resonant frequency f_1 (in reflection band), the series resonant circuit L_2C_2 is used to produce the higher resonant frequency f_2, and the capacitor C_t is used to create the transmission band frequency f_t. The normalized (with respect to the free-space impedance and admittance, respectively) inductive reactance X_{L1} and capacitive susceptance B_{C1} of the equivalent circuit model are given as follows:

$$X_{L_1} = \omega_1 L_1 = F(p,w,\lambda_1) = \frac{p}{\lambda_1}[-\ell n(\beta_w) + G(p,w,\lambda_1)], \tag{1}$$

where λ_1 and ω_1 are the wavelength and angular frequency of the first resonant frequency f_1, respectively:

$$G(p,w,\lambda_1) = \frac{1}{2}\times\frac{(1-\beta_w^2)^2[(1-\frac{\beta_w^4}{4})(A_{1+}+A_{1-})+4\beta_w^2 A_{1+}A_{1-}]}{(1-\frac{\beta_w^2}{4})+(\beta_w^2+\frac{\beta_w^4}{2}-\frac{\beta_w^6}{8})(A_{1+}+A_{1-})+2\beta_w^6 A_{1+}A_{1-}}, \tag{2}$$

$$A_{1+} = A_{1-} = \frac{1}{\sqrt{1-(\frac{p}{\lambda_1})^2}} - 1, \tag{3}$$

$$\beta_w = \sin(\frac{\pi w}{2p}), \tag{4}$$

$$\begin{aligned} B_{c_1} = \omega_1 C_1 &= \frac{4d}{p}F(p,s,\lambda_1) + \frac{4(2h+s)}{p}F(p,p-d,\lambda_1) \\ &= \frac{4d}{\lambda_1}[-\ell n(\beta_s) + G(p,s,\lambda_1)] \\ &+ \frac{4(2h+s)}{\lambda_1}[-\ell n(\beta_{pd}) + G(p,p-d,\lambda_1)], \end{aligned} \tag{5}$$

where

$$G(p,s,\lambda_1) = \frac{1}{2}\times\frac{(1-\beta_s^2)^2[(1-\frac{\beta_s^4}{4})(A_{1+}+A_{1-})+4\beta_s^2 A_{1+}A_{1-}]}{(1-\frac{\beta_s^2}{4})+(\beta_s^2+\frac{\beta_s^4}{2}-\frac{\beta_s^6}{8})(A_{1+}+A_{1-})+2\beta_s^6 A_{1+}A_{1-}}, \tag{6}$$

$$G(p,p-d,\lambda_1) = \frac{1}{2}\times\frac{(1-\beta_{pd}^2)^2[(1-\frac{\beta_{pd}^4}{4})(A_{1+}+A_{1-})+4\beta_{pd}^2 A_{1+}A_{1-}]}{(1-\frac{\beta_{pd}^2}{4})+(\beta_{pd}^2+\frac{\beta_{pd}^4}{2}-\frac{\beta_{pd}^6}{8})(A_{1+}+A_{1-})+2\beta_{pd}^6 A_{1+}A_{1-}}, \tag{7}$$

$$\beta_s = \sin(\frac{\pi s}{2p}), \tag{8}$$

$$\beta_{pd} = \sin[\frac{\pi \text{ (p-d)}}{2p}]. \tag{9}$$

The first resonant frequency f_1 can be obtained from L_1 and C_1 expressed by:

$$f_1 = \frac{1}{2\pi\sqrt{L_1C_1}}. \tag{10}$$

The normalized inductive reactance X_{L2} of the equivalent circuit model is given as following:

$$\begin{aligned} X_{L_2} = \omega_2 L_2 &= \frac{d}{2p}F(p,\ 2h+s,\lambda_2) + \frac{1}{2}F(\frac{p}{2},\ w,\lambda_2) \\ &= \frac{d}{2\lambda_2}[-\ell n(\beta_{hs}) + G(p,\ 2h+s,\lambda_2)] \\ &+ \frac{p}{4\lambda_2}[-\ell n(\beta_{p/2}) + G(\frac{p}{2},w,\lambda_2)], \end{aligned} \tag{11}$$

where λ_2 and ω_2 are the wavelength and angular frequency of the second resonant frequency f_2, respectively:

$$G(p,\ 2h+s,\lambda_2) = \frac{1}{2}\times\frac{(1-\beta_{hs}^2)^2[(1-\frac{\beta_{hs}^4}{4})(A_{2+}+A_{2-})+4\beta_{hs}^2 A_{2+}A_{2-}]}{(1-\frac{\beta_{hs}^2}{4})+(\beta_{hs}^2+\frac{\beta_{hs}^4}{2}-\frac{\beta_{hs}^6}{8})(A_{2+}+A_{2-})+2\beta_{hs}^6 A_{2+}A_{2-}}, \tag{12}$$

$$G(\frac{p}{2},\ w,\lambda_2) = \frac{1}{2}\times\frac{(1-\beta_{p2}^2)^2[(1-\frac{\beta_{p2}^4}{4})(A_{3+}+A_{3-})+4\beta_{p2}^2 A_{3+}A_{3-}]}{(1-\frac{\beta_{p2}^2}{4})+(\beta_{p2}^2+\frac{\beta_{p2}^4}{2}-\frac{\beta_{p2}^6}{8})(A_{3+}+A_{3-})+2\beta_{p2}^6 A_{3+}A_{3-}}, \tag{13}$$

$$A_{2+} = A_{2-} = \frac{1}{\sqrt{1-(\frac{p}{\lambda_2})^2}} - 1, \tag{14}$$

$$A_{3+} = A_{3-} = \frac{1}{\sqrt{1-(\frac{p}{2\lambda_2})^2}} - 1, \tag{15}$$

$$\beta_{hs} = \sin[\frac{\pi\ (2h+s)}{2p}], \tag{16}$$

$$\beta_{p2} = \sin(\frac{\pi\ \mathrm{w}}{p}). \tag{17}$$

The normalized capacitive susceptance B_{C2} of the equivalent circuit model is given as following:

$$\begin{aligned} B_{c_2} &= \omega_2 C_2 = \frac{8(2h+s)}{p} F(p, p-d, \lambda_2) \\ &= \frac{8(2h+s)}{\lambda_2}[-\ell n(\beta_{pd}) + G(p, p-d, \lambda_2)], \end{aligned} \tag{18}$$

where

$$G(p, p-d, \lambda_2)$$

$$= \frac{1}{2} \times \frac{(1-\beta_{pd}^2)^2[(1-\frac{\beta_{pd}^4}{4})(A_{2+}+A_{2-}) + 4\beta_{pd}^2 A_{2+}A_{2-}]}{(1-\frac{\beta_{pd}^2}{4}) + (\beta_{pd}^2 + \frac{\beta_{pd}^4}{2} - \frac{\beta_{pd}^6}{8})(A_{2+}+A_{2-}) + 2\beta_{pd}^6 A_{2+}A_{2-}}, \tag{19}$$

β_{pd}, A_{2+}, and A_{2-} are given in (9) and (14), respectively. The second resonant frequency f_2 can be obtained from L_2 and C_2 expressed by:

$$f_2 = \frac{1}{2\pi\sqrt{L_2 C_2}}. \tag{20}$$

Equations (1)-(20) are valid when $p<\lambda_2$ and $p>d$, where λ_2 is the wavelength of the second resonant frequency f_2. In band-stop electromagnetic shielding applications, the resonant frequencies f_1 and f_2 are specified first and then all parameters of the unit should be determined. However, to simultaneously determine all parameters of one Jerusalem-cross unit for arbitrarily given resonant frequencies f_1 and f_2 is not an easy job. In the following section, the least-square curve fitting technique will be applied to calculate all parameters of any Jerusalem-cross element for arbitrarily given dual resonant (rejection) frequencies f_1 and f_2.

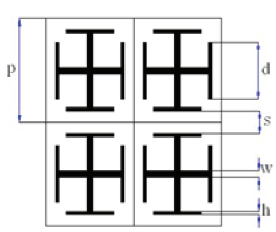

Fig. 1. Geometrical parameters of a FSS constructed with Jerusalem-cross grids.

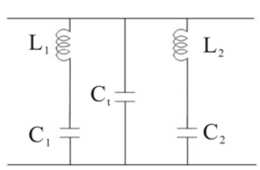

Fig. 2. An equivalent circuit model for Jerusalem-cross grids.

III. LEAST-SQUARE CURVE FITTING TECHNIQUE

The equivalent circuit model of a thin, continuous, and infinitely long array of Jerusalem-cross grids is presented in Fig. 2. In the band-stop electromagnetic shielding design, critical geometrical parameters of Jerusalem-cross grids p, w, s, h, and d should be solved for arbitrarily given dual resonant frequencies f_1 and f_2. Basically, resonant frequencies f_1 and f_2 are two nonlinear functions expressed by (10) and (20) in terms of geometrical parameters p, w, s, h, and d. The method of differential corrections, together with Newton's iterative method [40], can be used to fit the nonlinear functions f_1 and f_2. The differential corrections method approximates the nonlinear functions with a linear form that is more convenient to use for an iterative solution. By estimating approximate values of the unknown coefficients $A_1^{(0)}$, $A_2^{(0)}$, $A_3^{(0)}$, $A_4^{(0)}$, and $A_5^{(0)}$, and expanding (10) and (20) in a Taylor's series with only the first-order terms retained, we obtain:

$$\begin{aligned} f_1 &= f_1^{(0)} + \Delta A_1(\frac{\partial f_1}{\partial A_1})^{(0)} + \Delta A_2(\frac{\partial f_1}{\partial A_2})^{(0)} + \Delta A_3(\frac{\partial f_1}{\partial A_3})^{(0)} \\ &+ \Delta A_4(\frac{\partial f_1}{\partial A_4})^{(0)} + \Delta A_5(\frac{\partial f_1}{\partial A_5})^{(0)}, \end{aligned} \tag{21}$$

$$\begin{aligned} f_2 &= f_2^{(0)} + \Delta A_1(\frac{\partial f_2}{\partial A_1})^{(0)} + \Delta A_2(\frac{\partial f_2}{\partial A_2})^{(0)} + \Delta A_3(\frac{\partial f_2}{\partial A_3})^{(0)} \\ &+ \Delta A_4(\frac{\partial f_2}{\partial A_4})^{(0)} + \Delta A_5(\frac{\partial f_2}{\partial A_5})^{(0)}, \end{aligned} \tag{22}$$

where A_1=p, A_2=w, A_3=s, A_4=h, and A_5=d. The superscript (0) is used to indicate values obtained after substituting the first guess ($A_1^{(0)}$, $A_2^{(0)}$, $A_3^{(0)}$, $A_4^{(0)}$, and $A_5^{(0)}$), for the unknown parameters in (10) and (20). Equations (21) and (22) are two linear functions of the correction terms ΔA_1, ΔA_2, ΔA_3, ΔA_4, and ΔA_5, and hence the least-square curve fitting method can be used directly to determine these correction terms. The correction terms, when added to the first guess, give an improved approximation of the unknown coefficients, i.e., $A_1^{(1)} = A_1^{(0)} + \Delta A_1$, $A_2^{(1)} = A_2^{(0)} + \Delta A_2$, $A_3^{(1)} = A_3^{(0)} + \Delta A_3$, $A_4^{(1)} = A_4^{(0)} + \Delta A_4$, and $A_5^{(1)} = A_5^{(0)} + \Delta A_5$. When the improved estimates $A_1^{(1)}$, $A_2^{(1)}$, $A_3^{(1)}$, $A_4^{(1)}$, and $A_5^{(1)}$ are subsequently substituted as new estimates of the unknown coefficients, the Taylor's series reduces to:

$$\begin{aligned} f_1 &= f_1^{(1)} + \Delta A_1(\frac{\partial f_1}{\partial A_1})^{(1)} + \Delta A_2(\frac{\partial f_1}{\partial A_2})^{(1)} + \Delta A_3(\frac{\partial f_1}{\partial A_3})^{(1)} \\ &+ \Delta A_4(\frac{\partial f_1}{\partial A_4})^{(1)} + \Delta A_5(\frac{\partial f_1}{\partial A_5})^{(1)}, \end{aligned} \tag{23}$$

$$\begin{aligned} f_2 &= f_2^{(1)} + \Delta A_1(\frac{\partial f_2}{\partial A_1})^{(1)} + \Delta A_2(\frac{\partial f_2}{\partial A_2})^{(1)} + \Delta A_3(\frac{\partial f_2}{\partial A_3})^{(1)} \\ &+ \Delta A_4(\frac{\partial f_2}{\partial A_4})^{(1)} + \Delta A_5(\frac{\partial f_2}{\partial A_5})^{(1)}, \end{aligned} \tag{24}$$

where $f_1^{(1)}$ and $f_2^{(1)}$ as well as their derivatives are obtained by substituting the values of $A_1^{(1)}$, $A_2^{(1)}$, $A_3^{(1)}$, $A_4^{(1)}$, and $A_5^{(1)}$ in (10) and (20), respectively. Again, the correction terms ΔA_1, ΔA_2, ΔA_3, ΔA_4, and ΔA_5 are determined using the least-square curve fitting method. The procedure is continued until the solution converges to within a specified accuracy. The criterion of best fit of the technique of least-square curve fitting is that the sum of the squares of the errors be a minimum expressed by:

$$S = \sum_{i=1}^{N} \varepsilon_{i1}^2 + \sum_{i=1}^{N} \varepsilon_{i2}^2 = \text{minimum}, \tag{25}$$

where the term errors ε_{i1}^2 and ε_{i2}^2 mean the difference between the measured (observed) values of the first and second resonant frequencies $f_{1M}(i)$ and $f_{2M}(i)$ and computed values from (23) and (24) for the i^{th} case, respectively. N is the total number of cases. Substituting (23) and (24) into (25), the result yields:

$$S = \sum_{i=1}^{N} [f_{1M}(i) - f_1(i)]^2 + \sum_{i=1}^{N} [f_{2M}(i) - f_2(i)]^2. \tag{26}$$

A necessary condition that a minimum for the error function S exists is that the partial derivatives with respect to each of the correction terms ΔA_1, ΔA_2, ΔA_3, ΔA_4, and ΔA_5 be zero. For example, in the first iteration:

$$\begin{aligned} \frac{\partial S}{\partial(\Delta A_j)} &= -2\sum_{i=1}^{N} \left(\frac{\partial f_1}{\partial A_j}\right)^{(0)} \Big[f_{1M}(i) - f_1^{(0)} - \Delta A_1 \left(\frac{\partial f_1}{\partial A_1}\right)^{(0)} \\ &\quad - \Delta A_2 \left(\frac{\partial f_1}{\partial A_2}\right)^{(0)} - \Delta A_3 \left(\frac{\partial f_1}{\partial A_3}\right)^{(0)} - \Delta A_4 \left(\frac{\partial f_1}{\partial A_4}\right)^{(0)} \\ &\quad - \Delta A_5 \left(\frac{\partial f_1}{\partial A_5}\right)^{(0)} \Big] - 2\sum_{i=1}^{N} \left(\frac{\partial f_2}{\partial A_j}\right)^{(0)} \Big[f_{2M}(i) - f_2^{(0)} \\ &\quad - \Delta A_1 \left(\frac{\partial f_2}{\partial A_1}\right)^{(0)} - \Delta A_2 \left(\frac{\partial f_2}{\partial A_2}\right)^{(0)} - \Delta A_3 \left(\frac{\partial f_2}{\partial A_3}\right)^{(0)} \\ &\quad - \Delta A_4 \left(\frac{\partial f_2}{\partial A_4}\right)^{(0)} - \Delta A_5 \left(\frac{\partial f_2}{\partial A_5}\right)^{(0)} \Big] \\ &= 0, \end{aligned} \tag{27}$$

where j= 1, 2, 3, 4, and 5. Equation (27) can be expressed as a matrix equation. One can easily solve for the correction terms ΔA_1, ΔA_2, ΔA_3, ΔA_4, and ΔA_5 in (28) by Gaussian elimination method.

Equation (28) is a very sensitive equation because the partial derivatives of resonant frequencies f_1 and f_2 with respect to each of the parameters A_1=p, A_2=w, A_3=s, A_4=h, and A_5=d still can generate nonlinear functions such as square root, natural logarithm, sine, and cosine. Therefore, the values of parameters p, w, s, h, and d should be limited to an acceptable range in the Newton's iterative process. In order to obtain a stable iterative process, the parameters p, w, s, h, and d are automatically checked and set to $0.75\lambda_2 < p < \lambda_2$, $0.1\lambda_2 < w < 0.2\lambda_2$, $0.03\lambda_2 < s < 0.1\lambda_2$, $0.03\lambda_2 < h < 0.1\lambda_2$, and $0.4\lambda_2 < d < 0.7\lambda_2$ in each iteration, respectively:

$$\begin{bmatrix} \sum_{i=1}^{N}\left[\left(\frac{\partial f_1}{\partial A_1}\right)^{(0)}\right]^2 + \sum_{i=1}^{N}\left[\left(\frac{\partial f_2}{\partial A_1}\right)^{(0)}\right]^2 & \cdot & \cdot & \cdot & \sum_{i=1}^{N}\left(\frac{\partial f_1}{\partial A_1}\right)^{(0)}\left(\frac{\partial f_1}{\partial A_5}\right)^{(0)} + \sum_{i=1}^{N}\left(\frac{\partial f_2}{\partial A_1}\right)^{(0)}\left(\frac{\partial f_2}{\partial A_5}\right)^{(0)} \\ \sum_{i=1}^{N}\left(\frac{\partial f_1}{\partial A_2}\right)^{(0)}\left(\frac{\partial f_1}{\partial A_1}\right)^{(0)} + \sum_{i=1}^{N}\left(\frac{\partial f_2}{\partial A_2}\right)^{(0)}\left(\frac{\partial f_2}{\partial A_1}\right)^{(0)} & \cdots & & & \sum_{i=1}^{N}\left(\frac{\partial f_1}{\partial A_2}\right)^{(0)}\left(\frac{\partial f_1}{\partial A_5}\right)^{(0)} + \sum_{i=1}^{N}\left(\frac{\partial f_2}{\partial A_2}\right)^{(0)}\left(\frac{\partial f_2}{\partial A_5}\right)^{(0)} \\ \cdot & \cdot & \cdot & \cdot & \cdot \\ \cdot & \cdot & \cdot & \cdot & \cdot \\ \sum_{i=1}^{N}\left(\frac{\partial f_1}{\partial A_5}\right)^{(0)}\left(\frac{\partial f_1}{\partial A_1}\right)^{(0)} + \sum_{i=1}^{N}\left(\frac{\partial f_2}{\partial A_5}\right)^{(0)}\left(\frac{\partial f_2}{\partial A_1}\right)^{(0)} & \cdot & \cdot & \cdot & \sum_{i=1}^{N}\left[\left(\frac{\partial f_1}{\partial A_5}\right)^{(0)}\right]^2 + \sum_{i=1}^{N}\left[\left(\frac{\partial f_2}{\partial A_5}\right)^{(0)}\right]^2 \end{bmatrix}$$

$$\times \begin{bmatrix} \Delta A_1 \\ \Delta A_2 \\ \Delta A_3 \\ \Delta A_4 \\ \Delta A_5 \end{bmatrix} = \begin{bmatrix} \sum_{i=1}^{N}\left(\frac{\partial f_1}{\partial A_1}\right)^{(0)}[f_{1M}(i) - f_1^{(0)}] + \sum_{i=1}^{N}\left(\frac{\partial f_2}{\partial A_1}\right)^{(0)}[f_{2M}(i) - f_2^{(0)}] \\ \sum_{i=1}^{N}\left(\frac{\partial f_1}{\partial A_2}\right)^{(0)}[f_{1M}(i) - f_1^{(0)}] + \sum_{i=1}^{N}\left(\frac{\partial f_2}{\partial A_2}\right)^{(0)}[f_{2M}(i) - f_2^{(0)}] \\ \sum_{i=1}^{N}\left(\frac{\partial f_1}{\partial A_3}\right)^{(0)}[f_{1M}(i) - f_1^{(0)}] + \sum_{i=1}^{N}\left(\frac{\partial f_2}{\partial A_3}\right)^{(0)}[f_{2M}(i) - f_2^{(0)}] \\ \sum_{i=1}^{N}\left(\frac{\partial f_1}{\partial A_4}\right)^{(0)}[f_{1M}(i) - f_1^{(0)}] + \sum_{i=1}^{N}\left(\frac{\partial f_2}{\partial A_4}\right)^{(0)}[f_{2M}(i) - f_2^{(0)}] \\ \sum_{i=1}^{N}\left(\frac{\partial f_1}{\partial A_5}\right)^{(0)}[f_{1M}(i) - f_1^{(0)}] + \sum_{i=1}^{N}\left(\frac{\partial f_2}{\partial A_5}\right)^{(0)}[f_{2M}(i) - f_2^{(0)}] \end{bmatrix}. \tag{28}$$

The partial derivatives of resonant frequencies f_1 and f_2 with respect to each of the parameters can be obtained by the following two equations:

$$\frac{\partial f_1}{\partial A_i} = -\frac{1}{4\pi}(L_1 C_1)^{-\frac{3}{2}}(L_1 \frac{\partial C_1}{\partial A_i} + C_1 \frac{\partial L_1}{\partial A_i}), \quad (29)$$

$$\frac{\partial f_2}{\partial A_i} = -\frac{1}{4\pi}(L_2 C_2)^{-\frac{3}{2}}(L_2 \frac{\partial C_2}{\partial A_i} + C_2 \frac{\partial L_2}{\partial A_i}), \quad (30)$$

where A_1=p, A_2=w, A_3=s, A_4=h, and A_5=d. The partial derivatives of inductances and capacitances L_1, L_2, C_1, and C_2 are with respect to each of the parameters p, w, s, h, and d as shown in APPENDIX.

IV. VALIDATION OF LEAST-SQUARE CURVE FITTING

In order to validate the least-square curve fitting technique, dimensions of six Jerusalem-cross grids with thin, infinitely long, and perfectly conducting strips listed in the literature [38] are checked by the proposed technique. Simulation results of transmission for six Jerusalem-cross grids generated by the least-square curve fitting technique are studied by the commercial software package HFSS. Comparisons of two specific resonant frequencies f_1 and f_2 obtained by the least-square curve fitting technique, improved empirical model [38], and measurement [38] are listed in Table 1. Obviously, the six sets of dimensions obtained by the improved empirical model are different from those obtained by the least-square curve fitting technique. But it is found that simulation results of the resonant frequencies f_1 and f_2 for the six sets of parameters generated by the least-square curve fitting technique make a good agreement with those obtained by the empirical model and measurement available in the literature [38]. Table 1 illustrates that the set of dimensions of a Jerusalem-cross grid for any specific dual resonant frequencies f_1 and f_2 is not unique. Table 2 shows the comparison of computational time obtained by the least-square (LS) curve fitting technique and HFSS implemented with genetic algorithm (GA) [41] for design of Jerusalem-cross parameters in a personal computer. It is illustrated that the proposed method provides a fast solution for design of Jerusalem-cross parameters. The frequency responses of transmission of the six Jerusalem-cross grids, their dimensions obtained by the least-square curve fitting technique, are also shown in Figs. 3-8. These Jerusalem-cross grids have a transmission of more than -30 dB at resonant frequencies f_1 and f_2. The average bandwidths obtained at resonant frequencies f_1 and f_2 are more than 12% with a transmission of -10 dB.

Table 1: Comparisons of resonant frequencies f_1 and f_2 obtained by the least-square (LS) curve fitting technique (Figs. 3-8), improved empirical model (IEM) [38], and measurement (M) [38] for different Jerusalem-cross grids for normal wave incidence

No.	Dimensions (mm) [38]					Dimensions (mm) (LS)					f_1 (GHz)			f_2 (GHz)		
	p	w	d	h	s	p	w	d	h	s	M [38]	IEM [38]	LS	M [38]	IEM [38]	LS
1	5.82	0.8	4.05	0.4	0.3	7.05	1.06	3.63	0.23	0.24	14.1	14.0	14.9 (Fig. 3)	41.5	42.7	40.5 (Fig. 3)
2	5.82	0.8	4.6	0.42	0.27	7.11	0.82	3.9	0.73	0.28	12.8	12.8	12.6 (Fig. 4)	38.3	38.0	37.6 (Fig. 4)
3	6.5	0.9	4.95	0.3	0.21	7.86	0.92	4.5	0.86	0.3	11.6	11.3	10.9 (Fig. 5)	33.7	34.2	33.6 (Fig. 5)
4	5.84	1.42	4.5	0.32	0.38	5.96	0.82	3.70	0.39	0.53	17.3	17.0	17.0 (Fig. 6)	43.0	41.8	41.9 (Fig. 6)
5	6.3	1.18	4.8	0.39	0.41	6.7	0.94	4.15	0.41	0.40	14.3	14.2	14.5 (Fig. 7)	38.3	38.2	37.4 (Fig. 7)
6	5.98	1.18	4.6	0.42	0.38	7.00	1.0	3.75	0.35	0.34	14.9	15.0	14.8 (Fig. 8)	40.1	40.0	40.1 (Fig. 8)

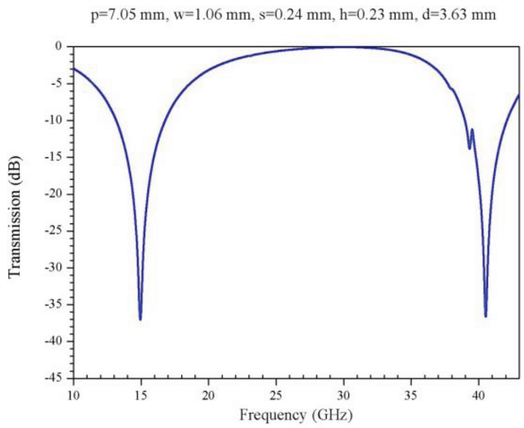

Fig. 3. The frequency response of transmission of the sample No. 1 listed in Table 1.

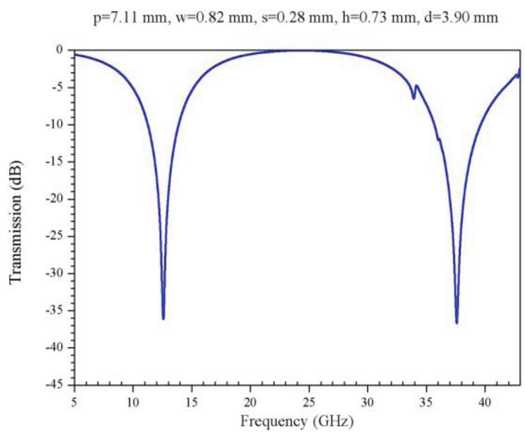

Fig. 4. The frequency response of transmission of the sample No. 2 listed in Table 1.

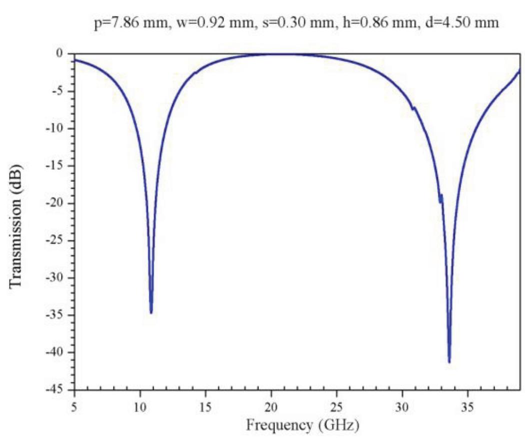

Fig. 5. The frequency response of transmission of the sample No. 3 listed in Table 1.

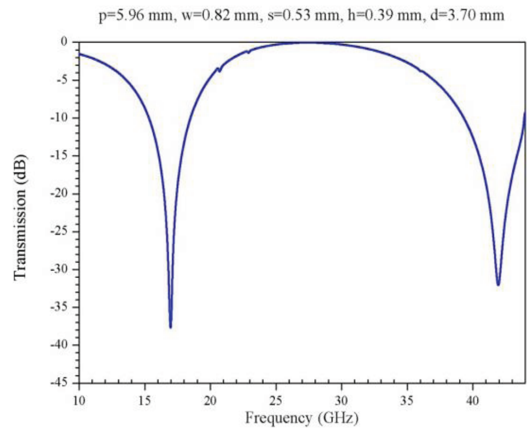

Fig. 6. The frequency response of transmission of the sample No. 4 listed in Table 1.

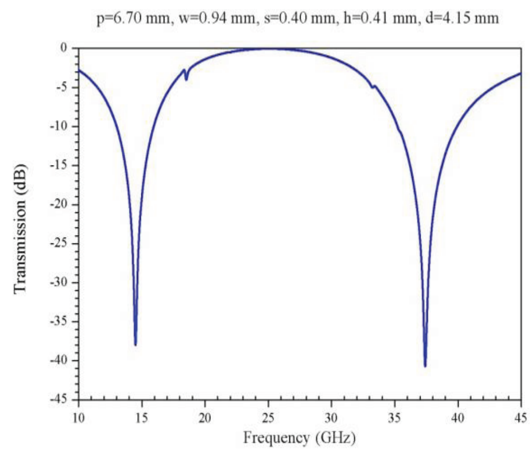

Fig. 7. The frequency response of transmission of the sample No. 5 listed in Table 1.

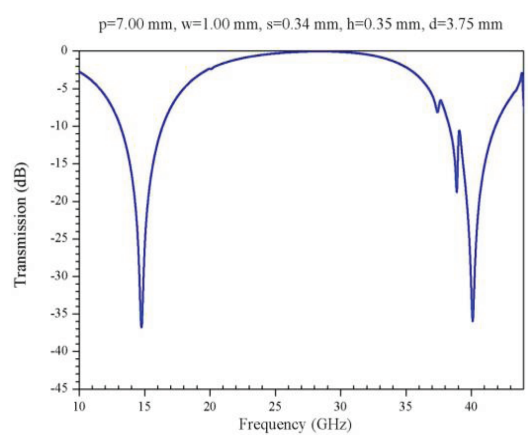

Fig. 8. The frequency response of transmission of the sample No. 6 listed in Table 1.

Table 2: Comparison of computational time obtained by the least-square (LS) curve fitting technique and HFSS implemented with genetic algorithm (GA) for design of Jerusalem-cross parameters

No.	LS	HFSS with GA
1	3 s	1 day 7 hr 27 m 21 s
2	8 s	2 day 18 hr 28 m 13 s
3	6 s	3 day 16 hr 45 m 17 s
4	13 s	4 day 13 hr 24 m 49 s
5	4 s	1 day 19 hr 14 m 29 s
6	9 s	3 day 23 hr 58 m 38 s

V. JERUSALEM-CROSS SLOTS

In order to improve EM transmission, aperture types of FSSs may be used to provide a better signal transmission at specific frequencies while also providing an isolation capability for unwanted EM noises. With all conducting and non-conducting areas interchanged, a Jerusalem-cross slot (a complementary Jerusalem-cross grid) can be used to reverse the transmission and reflection coefficients of the Jerusalem-cross grid [38]. We arbitrarily specify two pairs of dual resonant frequencies of (2.45, 5.8) and (3.96, 7.92) GHz to design two Jerusalem-cross slots by the least-square curve fitting technique. The Jerusalem-cross slots are constructed on a copper foil with a thickness of 0.05 mm. The specific frequencies of (2.45, 5.8) and (3.96, 7.92) GHz are in the Bluetooth (2.4-2.48 GHz), wireless local area network (IEEE802. 11a, upper band 5.725-5.825 GHz), and ultra-wideband (low-frequency band 3.168-4.752 GHz and high-frequency band 6.336-9.504 GHz) applications. Simulation results of reflection at frequencies (2.45, 5.8) and (3.96, 7.92) GHz will be investigated by checking the reflection with better than 10 dB return loss for the two Jerusalem-cross slots. The simulation results of frequency response of reflection will also be checked by measurement data. Measurement data of reflection of the two Jerusalem-cross slots are obtained by using an Anritsz37369C Vector Network Analyzer and a pair of horn antennas operating at frequencies of 1-18 GHz as shown in Fig. 9. The frequency responses of reflection of the first and second Jerusalem-cross slots with parameters (p=40.0 mm, w=5.4 mm, s=4.5 mm, h=2.1 mm, d=29.0 mm) and (p=28.5 mm, w=5.6 mm, s=3.8 mm, h=1.2 mm, d=21.6 mm) are shown in Figs. 10 and 11, respectively. From Figs. 10 and 11, it is shown that simulation results of frequency responses of reflection make a good agreement with those obtained by measurements. Figure 10 shows that the first Jerusalem-cross slot has a reflection of more than -30 dB at frequencies of 2.45 and 5.8 GHz. Simulation and measurement results of bandwidths at frequencies of 2.45 and 5.8 GHz have an average value of 15% with a reflection of -10 dB. From Fig. 11, the second Jerusalem-cross slot has a reflection of more than -40 dB at frequencies of 3.96 and 7.92 GHz. Simulation and measurement of bandwidths at frequencies of 3.96 and 7.92 GHz have an average value of 14.5% with a reflection of -10 dB. These bandwidths are enough to effectively transmit the Bluetooth, wireless local area network, and ultra-wideband signals.

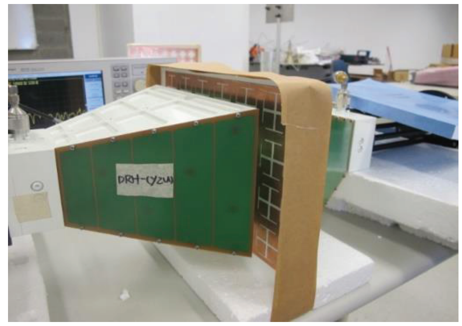

Fig. 9. Measurement setup.

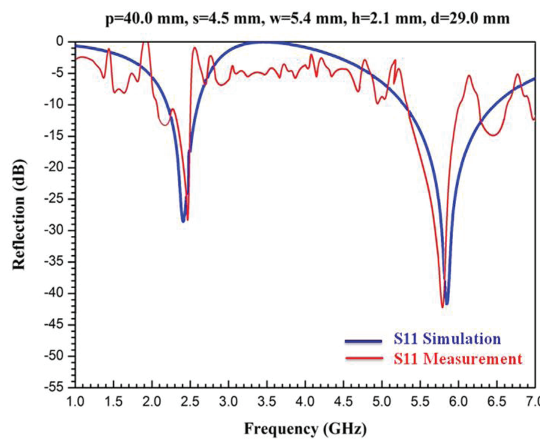

Fig. 10/ The frequency response of reflection of the first Jerusalem-cross slot.

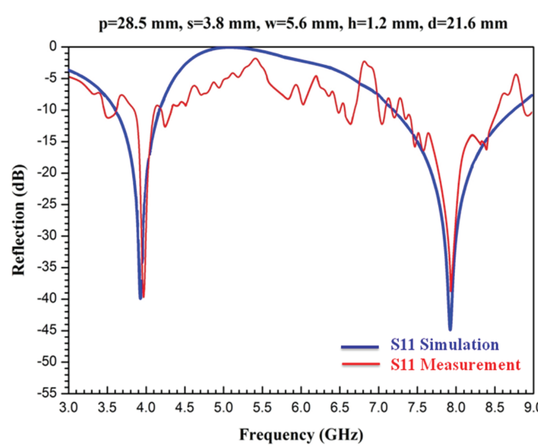

Fig. 11. The frequency response of reflection of the second Jerusalem-cross slot.

VI. CONCLUSION

In this paper, we propose the least-square curve fitting technique to quickly obtain optimum values of geometrical parameters of a dual-band Jerusalem-cross grid with thin, infinitely long, and perfectly conducting strips. Based on circuit model, the least-square curve fitting technique can provide a quick and accurate design of a dual-band Jerusalem-cross grid for arbitrarily specifying any dual resonant frequencies. The validity of the proposed technique has been checked by comparing two specific resonant frequencies f_1 and f_2 with those obtained by the improved empirical model and measurement method. The proposed method provides a fast solution for design of Jerusalem-cross parameters. The proposed technique can also be used to optimally design a dual-band Jerusalem-cross slot for arbitrarily specifying any two resonant frequencies. However, the proposed technique presented in this paper does not include the substrate. It is expected that the presence of the dielectric substrate will shift the resonant frequencies downwards. In the future works, the shifting factor will be further studied on the transmission and reflection of an energy-saving glass coated with a metallic oxide layer on one side of ordinary float glass which is widely used in modern building.

APPENDIX

This Appendix illustrates the partial derivatives of inductances and capacitances L_1, L_2, C_1, and C_2 with respect to each of the parameters p, w, s, h, and d as following:

$$\frac{\partial L_1}{\partial A_1}=\frac{\partial L_1}{\partial p}=\frac{1}{\omega_1\lambda_1}[-\ell n(\beta_w+G(p,w,\lambda_1)] + \frac{p}{\omega_1\lambda_1}[-\frac{1}{\beta_w}\frac{\partial \beta_w}{\partial p}+\frac{\partial G(p,w,\lambda_1)}{\partial p}], \tag{31}$$

where

$$\frac{\partial \beta_w}{\partial p}=-\frac{\pi w}{2p^2}\cos(\frac{\pi w}{2p}), \tag{32}$$

$$\frac{\partial G(p,w,\lambda_1)}{\partial p}=\frac{1}{2}\frac{G_d\frac{\partial G_n}{\partial p}-G_n\frac{\partial G_d}{\partial p}}{G_d^2}, \tag{33}$$

$$G_n=(1-\beta_w^2)^2[(1-\frac{\beta_w^4}{4})(A_{1+}+A_{1-})+4\beta_w^2A_{1+}A_{1-}], \tag{34}$$

$$G_d=(1-\frac{\beta_w^2}{4})+(\beta_w^2+\frac{\beta_w^4}{2}-\frac{\beta_w^6}{8})(A_{1+}+A_{1-})+2\beta_w^6A_{1+}A_{1-}, \tag{35}$$

$$\begin{aligned}\frac{\partial G_n}{\partial p}&=2(1-\beta_w^2)(-2\beta_w\frac{\partial \beta_w}{\partial p})[(1-\frac{\beta_w^4}{4})(A_{1+}+A_{1-})\\&+4\beta_w^2A_{1+}A_{1-}]+(1-\beta_w^2)^2[-\beta_w^3\frac{\partial \beta_w}{\partial p}(A_{1+}+A_{1-})\\&+(1-\frac{\beta_w^4}{4})(\frac{\partial A_{1+}}{\partial p}+\frac{\partial A_{1-}}{\partial p})+4\beta_w^2A_{1+}\frac{\partial A_{1-}}{\partial p}\\&+4\beta_w^2A_{1-}\frac{\partial A_{1+}}{\partial p}+8\beta_wA_{1+}A_{1-}\frac{\partial \beta_w}{\partial p}],\end{aligned} \tag{36}$$

$$\begin{aligned}\frac{\partial G_d}{\partial p}&=-\frac{1}{2}\beta_w\frac{\partial \beta_w}{\partial p}+(2\beta_w+2\beta_w^3-\frac{3}{4}\beta_w^5)\frac{\partial \beta_w}{\partial p}(A_{1+}+A_{1-})\\&+(\beta_w^2+\frac{\beta_w^4}{2}-\frac{\beta_w^6}{8})(\frac{\partial A_{1+}}{\partial p}+\frac{\partial A_{1-}}{\partial p})\\&+2\beta_w^6A_{1+}\frac{\partial A_{1-}}{\partial p}+2\beta_w^6A_{1-}\frac{\partial A_{1+}}{\partial p}\\&+12\beta_w^5A_{1+}A_{1-}\frac{\partial \beta_w}{\partial p},\end{aligned} \tag{37}$$

$$\frac{\partial A_{1+}}{\partial p}=\frac{\partial A_{1-}}{\partial p}=-\frac{1}{2}[1-(\frac{p}{\lambda_1})^2]^{-\frac{3}{2}}(\frac{2p}{\lambda_1^2}), \tag{38}$$

$$\frac{\partial L_1}{\partial A_2}=\frac{\partial L_1}{\partial w}=\frac{p}{\omega_1\lambda_1}[-\frac{1}{\beta_w}\frac{\partial \beta_w}{\partial w}+\frac{\partial G(p,w,\lambda_1)}{\partial w}], \tag{39}$$

where

$$\frac{\partial \beta_w}{\partial w}=\frac{\pi}{2p}\cos(\frac{\pi w}{2p}), \tag{40}$$

$$\frac{\partial G(p,w,\lambda_1)}{\partial w}=\frac{1}{2}\frac{G_d\frac{\partial G_n}{\partial w}-G_n\frac{\partial G_d}{\partial w}}{G_d^2}, \tag{41}$$

$$\begin{aligned}\frac{\partial G_n}{\partial w}&=2(1-\beta_w^2)(-2\beta_w\frac{\partial \beta_w}{\partial w})[(1-\frac{\beta_w^4}{4})(A_{1+}+A_{1-})\\&+4\beta_w^2A_{1+}A_{1-}]+(1-\beta_w^2)^2[-\beta_w^3\frac{\partial \beta_w}{\partial w}(A_{1+}+A_{1-})\\&+8\beta_wA_{1+}A_{1-}\frac{\partial \beta_w}{\partial w}],\end{aligned} \tag{42}$$

$$\begin{aligned}\frac{\partial G_d}{\partial w}&=-\frac{1}{2}\beta_w\frac{\partial \beta_w}{\partial w}\\&+(2\beta_w+2\beta_w^3-\frac{3}{4}\beta_w^5)\frac{\partial \beta_w}{\partial w}(A_{1+}+A_{1-})\\&+12\beta_w^5A_{1+}A_{1-}\frac{\partial \beta_w}{\partial w},\end{aligned} \tag{43}$$

$$\frac{\partial L_1}{\partial A_3}=\frac{\partial L_1}{\partial s}=0, \tag{44}$$

$$\frac{\partial L_1}{\partial A_4}=\frac{\partial L_1}{\partial h}=0, \tag{45}$$

$$\frac{\partial L_1}{\partial A_5}=\frac{\partial L_1}{\partial d}=0, \tag{46}$$

$$\begin{aligned}\frac{\partial C_1}{\partial A_1}=\frac{\partial C_1}{\partial p}&=\frac{4d}{\omega_1\lambda_1}[-\frac{1}{\beta_s}\frac{\partial \beta_s}{\partial p}+\frac{\partial G(p,s,\lambda_1)}{\partial p}\\&+\frac{4(2h+s)}{\omega_1\lambda_1}[-\frac{1}{\beta_{pd}}\frac{\partial \beta_{pd}}{\partial p}\\&+\frac{\partial G(p,p-d,\lambda_1)}{\partial p}],\end{aligned} \tag{47}$$

where

$$\frac{\partial \beta_s}{\partial p}=-\frac{\pi s}{2p^2}\cos(\frac{\pi s}{2p}), \tag{48}$$

$$\frac{\partial \beta_{pd}}{\partial p}=\frac{\pi d}{2p^2}\cos[\frac{\pi(p-d)}{2p}], \tag{49}$$

$$\frac{\partial G(p,s,\lambda_1)}{\partial p}=\frac{1}{2}\frac{G_{sd}\dfrac{\partial G_{sn}}{\partial p}-G_{sn}\dfrac{\partial G_{sd}}{\partial p}}{G_{sd}^2}, \quad (50)$$

$$G_{sn}=(1-\beta_s^2)^2[(1-\frac{\beta_s^4}{4})(A_{1+}+A_{1-})+4\beta_s^2A_{1+}A_{1-}], \quad (51)$$

$$\begin{aligned}G_{sd}&=(1-\frac{\beta_s^2}{4})+(\beta_s^2+\frac{\beta_s^4}{2}-\frac{\beta_s^6}{8})(A_{1+}+A_{1-})\\&+2\beta_s^6A_{1+}A_{1-},\end{aligned} \quad (52)$$

$$\begin{aligned}\frac{\partial G_{sn}}{\partial p}&=2(1-\beta_s^2)(-2\beta_s\frac{\partial\beta_s}{\partial p})[(1-\frac{\beta_s^4}{4})(A_{1+}+A_{1-})\\&+4\beta_s^2A_{1+}A_{1-}]+(1-\beta_s^2)^2[-\beta_s^3\frac{\partial\beta_s}{\partial p}(A_{1+}+A_{1-})\\&+(1-\frac{\beta_s^4}{4})(\frac{\partial A_{1+}}{\partial p}+\frac{\partial A_{1-}}{\partial p})+4\beta_s^2A_{1+}\frac{\partial A_{1-}}{\partial p}\\&+4\beta_s^2A_{1-}\frac{\partial A_{1+}}{\partial p}+8\beta_sA_{1+}A_{1-}\frac{\partial\beta_s}{\partial p}],\end{aligned} \quad (53)$$

$$\begin{aligned}\frac{\partial G_{sd}}{\partial p}&=-\frac{1}{2}\beta_s\frac{\partial\beta_s}{\partial p}\\&+(2\beta_s+2\beta_s^3-\frac{3}{4}\beta_s^5)\frac{\partial\beta_s}{\partial p}(A_{1+}+A_{1-})\\&+(\beta_s^2+\frac{\beta_s^4}{2}-\frac{\beta_s^6}{8})(\frac{\partial A_{1+}}{\partial p}+\frac{\partial A_{1-}}{\partial p})\\&+2\beta_s^6A_{1+}\frac{\partial A_{1-}}{\partial p}+2\beta_s^6A_{1-}\frac{\partial A_{1+}}{\partial p}\\&+12\beta_s^5A_{1+}A_{1-}\frac{\partial\beta_s}{\partial p},\end{aligned} \quad (54)$$

$$\frac{\partial G(p,p-d,\lambda_1)}{\partial p}=\frac{1}{2}\frac{G_{pdd}\dfrac{\partial G_{pdn}}{\partial p}-G_{pdn}\dfrac{\partial G_{pdd}}{\partial p}}{G_{pdd}^2}, \quad (55)$$

$$G_{pdn}=(1-\beta_{pd}^2)^2[(1-\frac{\beta_{pd}^4}{4})(A_{1+}+A_{1-})+4\beta_{pd}^2A_{1+}A_{1-}], \quad (56)$$

$$\begin{aligned}G_{pdd}&=(1-\frac{\beta_{pd}^2}{4})+(\beta_{pd}^2+\frac{\beta_{pd}^4}{2}-\frac{\beta_{pd}^6}{8})(A_{1+}+A_{1-})\\&+2\beta_{pd}^6A_{1+}A_{1-},\end{aligned} \quad (57)$$

$$\begin{aligned}\frac{\partial G_{pdn}}{\partial p}&=2(1-\beta_{pd}^2)(-2\beta_{pd}\frac{\partial\beta_{pd}}{\partial p})[(1-\frac{\beta_{pd}^4}{4})(A_{1+}+A_{1-})\\&+4\beta_{pd}^2A_{1+}A_{1-}]+(1-\beta_{pd}^2)^2[-\beta_{pd}^3\frac{\partial\beta_{pd}}{\partial p}(A_{1+}+A_{1-})\\&+(1-\frac{\beta_{pd}^4}{4})(\frac{\partial A_{1+}}{\partial p}+\frac{\partial A_{1-}}{\partial p})\ +4\beta_{pd}^2A_{1+}\frac{\partial A_{1-}}{\partial p}\\&+4\beta_{pd}^2A_{1-}\frac{\partial A_{1+}}{\partial p}+8\beta_{pd}A_{1+}A_{1-}\frac{\partial\beta_{pd}}{\partial p}],\end{aligned} \quad (58)$$

$$\begin{aligned}\frac{\partial G_{pdd}}{\partial p}&=-\frac{1}{2}\beta_{pd}\frac{\partial\beta_{pd}}{\partial p}\\&+(2\beta_{pd}+2\beta_{pd}^3-\frac{3}{4}\beta_{pd}^5)\frac{\partial\beta_{pd}}{\partial p}(A_{1+}+A_{1-})\\&+(\beta_{pd}^2+\frac{\beta_{pd}^4}{2}-\frac{\beta_{pd}^6}{8})(\frac{\partial A_{1+}}{\partial p}+\frac{\partial A_{1-}}{\partial p})\\&+2\beta_{pd}^6A_{1+}\frac{\partial A_{1-}}{\partial p}+2\beta_{pd}^6A_{1-}\frac{\partial A_{1+}}{\partial p}\\&+12\beta_{pd}^5A_{1+}A_{1-}\frac{\partial\beta_{pd}}{\partial p},\end{aligned} \quad (59)$$

$$\frac{\partial C_1}{\partial A_2}=\frac{\partial C_1}{\partial w}=0, \quad (60)$$

$$\begin{aligned}\frac{\partial C_1}{\partial A_3}=\frac{\partial C_1}{\partial s}&=\frac{4d}{\omega_1\lambda_1}[-\frac{1}{\beta_s}\frac{\partial\beta_s}{\partial s}+\frac{\partial G(p,s,\lambda_1)}{\partial s}\\&+\frac{4}{\omega_1\lambda_1}[-\ell n(\beta_{pd})+G(p,p-d,\lambda_1)],\end{aligned} \quad (61)$$

where

$$\frac{\partial\beta_s}{\partial s}=\frac{\pi s}{2p}\cos(\frac{\pi s}{2p}), \quad (62)$$

$$\frac{\partial G(p,s,\lambda_1)}{\partial s}=\frac{1}{2}\frac{G_{sd}\dfrac{\partial G_{sn}}{\partial s}-G_{sn}\dfrac{\partial G_{sd}}{\partial s}}{G_{sd}^2}, \quad (63)$$

$$\begin{aligned}\frac{\partial G_{sn}}{\partial s}&=2(1-\beta_s^2)(-2\beta_s\frac{\partial\beta_s}{\partial s})[(1-\frac{\beta_s^4}{4})(A_{1+}+A_{1-})\\&+4\beta_s^2A_{1+}A_{1-}]+(1-\beta_s^2)^2[-\beta_s^3\frac{\partial\beta_s}{\partial s}(A_{1+}+A_{1-})\\&+8\beta_sA_{1+}A_{1-}\frac{\partial\beta_s}{\partial s}],\end{aligned} \quad (64)$$

$$\begin{aligned}\frac{\partial G_{sd}}{\partial s}&=-\frac{1}{2}\beta_s\frac{\partial\beta_s}{\partial s}\\&+(2\beta_s+2\beta_s^3-\frac{3}{4}\beta_s^5)\frac{\partial\beta_s}{\partial s}(A_{1+}+A_{1-})\\&+12\beta_s^5A_{1+}A_{1-}\frac{\partial\beta_s}{\partial s},\end{aligned} \quad (65)$$

$$\frac{\partial C_1}{\partial A_4}=\frac{\partial C_1}{\partial h}=\frac{8}{\omega_1\lambda_1}[-\ell n(\beta_{pd})+G(p,p-d,\lambda_1)], \quad (66)$$

$$\begin{aligned}\frac{\partial C_1}{\partial A_5}&=\frac{\partial C_1}{\partial d}\\&=\frac{4(2h+s)}{\omega_1\lambda_1}[-\frac{1}{\beta_{pd}}\frac{\partial\beta_{pd}}{\partial d}+\frac{\partial G(p,p-d,\lambda_1)}{\partial d}],\end{aligned} \quad (67)$$

where

$$\frac{\partial\beta_{pd}}{\partial d}=\frac{-\pi}{2p}\cos[\frac{\pi(p-d)}{2p}], \quad (68)$$

$$\frac{\partial G(p,p-d,\lambda_1)}{\partial d}=\frac{1}{2}\frac{G_{pdd}\frac{\partial G_{pdn}}{\partial d}-G_{pdn}\frac{\partial G_{pdd}}{\partial d}}{G_{pdd}^2}, \tag{69}$$

$$\begin{aligned}\frac{\partial G_{pdn}}{\partial d}&=2(1-\beta_{pd}^2)(-2\beta_{pd}\frac{\partial\beta_{pd}}{\partial d})[(1-\frac{\beta_{pd}^4}{4})(A_{1+}+A_{1-})\\&+4\beta_{pd}^2A_{1+}A_{1-}]+(1-\beta_{pd}^2)^2[-\beta_{pd}^3\frac{\partial\beta_{pd}}{\partial d}(A_{1+}+A_{1-})\\&+8\beta_{pd}A_{1+}A_{1-}\frac{\partial\beta_{pd}}{\partial d}],\end{aligned} \tag{70}$$

$$\begin{aligned}\frac{\partial G_{pdd}}{\partial d}&=-\frac{1}{2}\beta_{pd}\frac{\partial\beta_{pd}}{\partial d}\\&+(2\beta_{pd}+2\beta_{pd}^3-\frac{3}{4}\beta_{pd}^5)\frac{\partial\beta_{pd}}{\partial d}(A_{1+}+A_{1-})\\&+12\beta_{pd}^5A_{1+}A_{1-}\frac{\partial\beta_{pd}}{\partial d},\end{aligned} \tag{71}$$

$$\begin{aligned}\frac{\partial L_2}{\partial A_1}=\frac{\partial L_2}{\partial p}&=\frac{d}{2\omega_2\lambda_2}[-\frac{1}{\beta_{hs}}\frac{\partial\beta_{hs}}{\partial p}+\frac{\partial G(p,2h+s,\lambda_2)}{\partial p}]\\&+\frac{1}{4\omega_2\lambda_2}[-\ell n(\beta_{p2}+G(\frac{p}{2},w,\lambda_2)]\\&+\frac{p}{4\omega_2\lambda_2}[-\frac{1}{\beta_{p2}}\frac{\partial\beta_{p2}}{\partial p}+\frac{\partial G(\frac{p}{2},w,\lambda_2)}{\partial p}],\end{aligned} \tag{72}$$

where

$$\frac{\partial\beta_{hs}}{\partial p}=-\frac{\pi(2h+s)}{2p^2}\cos[\frac{\pi(2h+s)}{2p}], \tag{73}$$

$$\frac{\partial\beta_{p2}}{\partial p}=-\frac{\pi w}{p^2}\cos[\frac{\pi w}{p}], \tag{74}$$

$$\frac{\partial G(p,\ 2h+s,\lambda_2)}{\partial p}=\frac{1}{2}\frac{G_{hsd}\frac{\partial G_{hsn}}{\partial p}-G_{hsn}\frac{\partial G_{hsd}}{\partial p}}{G_{hsd}^2}, \tag{75}$$

$$\begin{aligned}G_{hsn}&=(1-\beta_{hs}^2)^2[(1-\frac{\beta_{hs}^4}{4})(A_{2+}+A_{2-})\\&+4\beta_{hs}^2A_{2+}A_{2-}],\end{aligned} \tag{76}$$

$$\begin{aligned}G_{hsd}&=(1-\frac{\beta_{hs}^2}{4})+(\beta_{hs}^2+\frac{\beta_{hs}^4}{2}-\frac{\beta_{hs}^6}{8})(A_{2+}+A_{2-})\\&+2\beta_{hs}^6A_{2+}A_{2-},\end{aligned} \tag{77}$$

$$\begin{aligned}\frac{\partial G_{hsn}}{\partial p}&=2(1-\beta_{hs}^2)(-2\beta_{hs}\frac{\partial\beta_{hs}}{\partial p})[(1-\frac{\beta_{hs}^4}{4})(A_{2+}+A_{2-})\\&+4\beta_{hs}^2A_{2+}A_{2-}]+(1-\beta_{hs}^2)^2[-\beta_{hs}^3\frac{\partial\beta_{hs}}{\partial p}(A_{2+}+A_{2-})\\&+(1-\frac{\beta_{hs}^4}{4})(\frac{\partial A_{2+}}{\partial p}+\frac{\partial A_{2-}}{\partial p})+4\beta_{hs}^2A_{2+}\frac{\partial A_{2-}}{\partial p}\\&+4\beta_{hs}^2A_{2-}\frac{\partial A_{2+}}{\partial p}+8\beta_{hs}A_{2+}A_{2-}\frac{\partial\beta_{hs}}{\partial p}],\end{aligned} \tag{78}$$

$$\begin{aligned}\frac{\partial G_{hsd}}{\partial p}&=-\frac{1}{2}\beta_{hs}\frac{\partial\beta_{hs}}{\partial p}\\&+(2\beta_{hs}+2\beta_{hs}^3-\frac{3}{4}\beta_{hs}^5)\frac{\partial\beta_{hs}}{\partial p}(A_{2+}+A_{2-})\\&+(\beta_{hs}^2+\frac{\beta_{hs}^4}{2}-\frac{\beta_{hs}^6}{8})(\frac{\partial A_{2+}}{\partial p}+\frac{\partial A_{2-}}{\partial p})\\&+2\beta_{hs}^6A_{2+}\frac{\partial A_{2-}}{\partial p}+2\beta_{hs}^6A_{2-}\frac{\partial A_{2+}}{\partial p}\\&+12\beta_{hs}^5A_{2+}A_{2-}\frac{\partial\beta_{hs}}{\partial p},\end{aligned} \tag{79}$$

$$\frac{\partial A_{2+}}{\partial p}=\frac{\partial A_{2-}}{\partial p}=-\frac{1}{2}[1-(\frac{p}{\lambda_2})^2]^{-\frac{3}{2}}(\frac{2p}{\lambda_2^2}), \tag{80}$$

$$\frac{\partial G(\frac{p}{2},w,\lambda_2)}{\partial p}=\frac{1}{2}\frac{G_{p2wd}\frac{\partial G_{p2wn}}{\partial p}-G_{p2wn}\frac{\partial G_{p2wd}}{\partial p}}{G_{p2wd}^2}, \tag{81}$$

$$\begin{aligned}G_{p2wn}&=(1-\beta_{p2}^2)^2[(1-\frac{\beta_{p2}^4}{4})(A_{3+}+A_{3-})\\&+4\beta_{p2}^2A_{3+}A_{3-}],\end{aligned} \tag{82}$$

$$\begin{aligned}G_{p2wd}&=(1-\frac{\beta_{p2}^2}{4})\\&+(\beta_{p2}^2+\frac{\beta_{p2}^4}{2}-\frac{\beta_{p2}^6}{8})(A_{3+}+A_{3-})\\&+2\beta_{p2}^6A_{3+}A_{3-},\end{aligned} \tag{83}$$

$$\begin{aligned}\frac{\partial G_{p2wn}}{\partial p}&=2(1-\beta_{p2}^2)(-2\beta_{p2}\frac{\partial\beta_{p2}}{\partial p})[(1-\frac{\beta_{p2}^4}{4})(A_{3+}+A_{3-})\\&+4\beta_{p2}^2A_{2+}A_{2-}]+(1-\beta_{p2}^2)^2[-\beta_{p2}^3\frac{\partial\beta_{p2}}{\partial p}(A_{3+}+A_{3-})\\&+(1-\frac{\beta_{p2}^4}{4})(\frac{\partial A_{3+}}{\partial p}+\frac{\partial A_{3-}}{\partial p})\\&+4\beta_{p2}^2A_{3+}\frac{\partial A_{3-}}{\partial p}+4\beta_{p2}^2A_{3-}\frac{\partial A_{3+}}{\partial p}\\&+8\beta_{p2}A_{3+}A_{3-}\frac{\partial\beta_{p2}}{\partial p}],\end{aligned} \tag{84}$$

$$\begin{aligned}\frac{\partial G_{p2wd}}{\partial p}&=-\frac{1}{2}\beta_{p2}\frac{\partial\beta_{p2}}{\partial p}\\&+(2\beta_{p2}+2\beta_{p2}^3-\frac{3}{4}\beta_{p2}^5)\frac{\partial\beta_{p2}}{\partial p}(A_{3+}+A_{3-})\\&+(\beta_{p2}^2+\frac{\beta_{p2}^4}{2}-\frac{\beta_{p2}^6}{8})(\frac{\partial A_{3+}}{\partial p}+\frac{\partial A_{3-}}{\partial p})\\&+2\beta_{p2}^6A_{3+}\frac{\partial A_{3-}}{\partial p}+2\beta_{p2}^6A_{3-}\frac{\partial A_{3+}}{\partial p}\\&+12\beta_{p2}^5A_{3+}A_{3-}\frac{\partial\beta_{p2}}{\partial p},\end{aligned} \tag{85}$$

$$\frac{\partial A_{3+}}{\partial p} = \frac{\partial A_{3-}}{\partial p} = -\frac{1}{2}[1-(\frac{p}{2\lambda_2})^2]^{-\frac{3}{2}}(\frac{p}{2\lambda_2^2}), \quad (86)$$

$$\frac{\partial L_2}{\partial A_2} = \frac{\partial L_2}{\partial w} = \frac{p}{4\omega_2\lambda_2}[-\frac{1}{\beta_{p2}}\frac{\partial \beta_{p2}}{\partial w} + \frac{\partial G(\frac{p}{2}, w, \lambda_2)}{\partial w}], \quad (87)$$

where

$$\frac{\partial \beta_{p2}}{\partial w} = \frac{\pi w}{p}\cos[\frac{\pi w}{p}], \quad (88)$$

$$\frac{\partial G(\frac{p}{2}, w, \lambda_2)}{\partial w} = \frac{1}{2}\frac{G_{p2wd}\frac{\partial G_{p2wn}}{\partial w} - G_{p2wn}\frac{\partial G_{p2wd}}{\partial w}}{G_{p2wd}^2}, \quad (89)$$

$$\begin{aligned}\frac{\partial G_{p2wn}}{\partial w} &= 2(1-\beta_{p2}^2)(-2\beta_{p2}\frac{\partial \beta_{p2}}{\partial w})[(1-\frac{\beta_{p2}^4}{4})(A_{3+}+A_{3-}) \\ &+4\beta_{p2}^2 A_{2+}A_{2-}] \\ &+(1-\beta_{p2}^2)^2[-\beta_{p2}^3\frac{\partial \beta_{p2}}{\partial w}(A_{3+}+A_{3-}) \\ &+8\beta_{p2}A_{3+}A_{3-}\frac{\partial \beta_{p2}}{\partial w}],\end{aligned} \quad (90)$$

$$\begin{aligned}\frac{\partial G_{p2wd}}{\partial w} &= -\frac{1}{2}\beta_{p2}\frac{\partial \beta_{p2}}{\partial w} \\ &+(2\beta_{p2}+2\beta_{p2}^3-\frac{3}{4}\beta_{p2}^5)\frac{\partial \beta_{p2}}{\partial w}(A_{3+}+A_{3-}) \\ &+12\beta_{p2}^5 A_{3+}A_{3-}\frac{\partial \beta_{p2}}{\partial w},\end{aligned} \quad (91)$$

$$\frac{\partial L_2}{\partial A_3} = \frac{\partial L_2}{\partial s} = \frac{d}{2\omega_2\lambda_2}[-\frac{1}{\beta_{hs}}\frac{\partial \beta_{hs}}{\partial s} + \frac{\partial G(p, 2h+s, \lambda_2)}{\partial s}], \quad (92)$$

where

$$\frac{\partial \beta_{hs}}{\partial s} = \frac{\pi}{2p}\cos[\frac{\pi(2h+s)}{p}], \quad (93)$$

$$\frac{\partial G(p,\ 2h+s, \lambda_2)}{\partial s} = \frac{1}{2}\frac{G_{hsd}\frac{\partial G_{hsn}}{\partial s} - G_{hsn}\frac{\partial G_{hsd}}{\partial s}}{G_{hsd}^2}, \quad (94)$$

$$\begin{aligned}\frac{\partial G_{hsn}}{\partial s} &= 2(1-\beta_{hs}^2)(-2\beta_{hs}\frac{\partial \beta_{hs}}{\partial s})[(1-\frac{\beta_{hs}^4}{4})(A_{2+}+A_{2-}) \\ &+4\beta_{hs}^2 A_{2+}A_{2-}]+(1-\beta_{hs}^2)^2[-\beta_{hs}^3\frac{\partial \beta_{hs}}{\partial s}(A_{2+}+A_{2-}) \\ &+8\beta_{hs}A_{2+}A_{2-}\frac{\partial \beta_{hs}}{\partial s}],\end{aligned} \quad (95)$$

$$\begin{aligned}\frac{\partial G_{hsd}}{\partial s} &= -\frac{1}{2}\beta_{hs}\frac{\partial \beta_{hs}}{\partial s} \\ &+(2\beta_{hs}+2\beta_{hs}^3-\frac{3}{4}\beta_{hs}^5)\frac{\partial \beta_{hs}}{\partial s}(A_{2+}+A_{2-}) \\ &+12\beta_{hs}^5 A_{2+}A_{2-}\frac{\partial \beta_{hs}}{\partial s},\end{aligned} \quad (96)$$

$$\begin{aligned}\frac{\partial L_2}{\partial A_4} &= \frac{\partial L_2}{\partial h} \\ &= \frac{d}{2\omega_2\lambda_2}[-\frac{1}{\beta_{hs}}\frac{\partial \beta_{hs}}{\partial h} + \frac{\partial G(p,\ 2h+s, \lambda_2)}{\partial h}],\end{aligned} \quad (97)$$

where

$$\frac{\partial \beta_{hs}}{\partial h} = \frac{\pi}{p}\cos[\frac{\pi(2h+s)}{p}], \quad (98)$$

$$\frac{\partial G(p,\ 2h+s, \lambda_2)}{\partial h} = \frac{1}{2}\frac{G_{hsd}\frac{\partial G_{hsn}}{\partial h} - G_{hsn}\frac{\partial G_{hsd}}{\partial h}}{G_{hsd}^2}, \quad (99)$$

$$\begin{aligned}\frac{\partial G_{hsn}}{\partial h} &= 2(1-\beta_{hs}^2)(-2\beta_{hs}\frac{\partial \beta_{hs}}{\partial h})[(1-\frac{\beta_{hs}^4}{4})(A_{2+}+A_{2-}) \\ &+4\beta_{hs}^2 A_{2+}A_{2-}]+(1-\beta_{hs}^2)^2[-\beta_{hs}^3\frac{\partial \beta_{hs}}{\partial h}(A_{2+}+A_{2-}) \\ &+8\beta_{hs}A_{2+}A_{2-}\frac{\partial \beta_{hs}}{\partial h}]\end{aligned} \quad (100)$$

$$\begin{aligned}\frac{\partial G_{hsd}}{\partial h} &= -\frac{1}{2}\beta_{hs}\frac{\partial \beta_{hs}}{\partial h} \\ &+(2\beta_{hs}+2\beta_{hs}^3-\frac{3}{4}\beta_{hs}^5)\frac{\partial \beta_{hs}}{\partial h}(A_{2+}+A_{2-}) \\ &+12\beta_{hs}^5 A_{2+}A_{2-}\frac{\partial \beta_{hs}}{\partial h},\end{aligned} \quad (101)$$

$$\frac{\partial L_2}{\partial A_5} = \frac{\partial L_2}{\partial d} = \frac{d}{2\omega_2\lambda_2}[-\ell n(\beta_{hs}) + G(p,\ 2h+s, \lambda_2)], \quad (102)$$

$$\begin{aligned}\frac{\partial C_2}{\partial A_1} &= \frac{\partial C_2}{\partial p} \\ &= \frac{8(2h+s)}{\omega_2\lambda_2}[-\frac{1}{\beta_{pd}}\frac{\partial \beta_{pd}}{\partial p} + \frac{\partial G(p, p-d, \lambda_2)}{\partial p}],\end{aligned} \quad (103)$$

where

$$\frac{\partial G(p, p-d, \lambda_2)}{\partial p} = \frac{1}{2}\frac{G_{pdd2}\frac{\partial G_{pdn2}}{\partial p} - G_{pdn2}\frac{\partial G_{pdd2}}{\partial p}}{G_{pdd2}^2}, \quad (104)$$

$$\frac{\partial G_{pdn2}}{\partial p} = 2(1-\beta_{pd}^2)(-2\beta_{pd}\frac{\partial \beta_{pd}}{\partial p})[(1-\frac{\beta_{pd}^4}{4})(A_{2+}+A_{2-}) + 4\beta_{pd}^2 A_{2+}A_{2-}] + (1-\beta_{pd}^2)^2[-\beta_{pd}^3\frac{\partial \beta_{pd}}{\partial p}(A_{2+}+A_{2-}) + (1-\frac{\beta_{pd}^4}{4})(\frac{\partial A_{2+}}{\partial p}+\frac{\partial A_{2-}}{\partial p}) + 4\beta_{pd}^2 A_{2+}\frac{\partial A_{2-}}{\partial p} + 4\beta_{pd}^2 A_{2-}\frac{\partial A_{2+}}{\partial p} + 8\beta_{pd}A_{2+}A_{2-}\frac{\partial \beta_{pd}}{\partial p}], \quad (105)$$

$$\frac{\partial G_{pdd2}}{\partial p} = -\frac{1}{2}\beta_{pd}\frac{\partial \beta_{pd}}{\partial p} + (2\beta_{pd}+2\beta_{pd}^3-\frac{3}{4}\beta_{pd}^5)\frac{\partial \beta_{pd}}{\partial p}(A_{2+}+A_{2-}) + (\beta_{pd}^2+\frac{\beta_{pd}^4}{2}-\frac{\beta_{pd}^6}{8})(\frac{\partial A_{2+}}{\partial p}+\frac{\partial A_{2-}}{\partial p}) + 2\beta_{pd}^6 A_{2+}\frac{\partial A_{2-}}{\partial p} + 2\beta_{pd}^6 A_{2-}\frac{\partial A_{2+}}{\partial p} + 12\beta_{pd}^5 A_{2+}A_{2-}\frac{\partial \beta_{pd}}{\partial p}, \quad (106)$$

$$\frac{\partial C_2}{\partial A_2} = \frac{\partial C_2}{\partial w} = 0, \quad (107)$$

$$\frac{\partial C_2}{\partial A_3} = \frac{\partial C_2}{\partial s} = \frac{8}{\omega_2\lambda_2}[-\ell n(\beta_{pd}) + G(p, p-d, \lambda_2)], \quad (108)$$

$$\frac{\partial C_2}{\partial A_4} = \frac{\partial C_2}{\partial h} = \frac{16}{\omega_2\lambda_2}[-\ell n(\beta_{pd}) + G(p, p-d, \lambda_2)], \quad (109)$$

$$\frac{\partial C_2}{\partial A_5} = \frac{\partial C_2}{\partial d} = \frac{8(2h+s)}{\omega_2\lambda_2}[-\frac{1}{\beta_{pd}}\frac{\partial \beta_{pd}}{\partial d} + \frac{\partial G(p, p-d, \lambda_2)}{\partial d}], \quad (110)$$

where

$$\frac{\partial G(p, p-d, \lambda_2)}{\partial d} = \frac{1}{2}\frac{G_{pdd2}\frac{\partial G_{pdn2}}{\partial d} - G_{pdn2}\frac{\partial G_{pdd2}}{\partial d}}{G_{pdd2}^2}, \quad (111)$$

$$\frac{\partial G_{pdn2}}{\partial d} = 2(1-\beta_{pd}^2)(-2\beta_{pd}\frac{\partial \beta_{pd}}{\partial d})[(1-\frac{\beta_{pd}^4}{4})(A_{2+}+A_{2-}) + 4\beta_{pd}^2 A_{2+}A_{2-}] + (1-\beta_{pd}^2)^2[-\beta_{pd}^3\frac{\partial \beta_{pd}}{\partial d}(A_{2+}+A_{2-}) + 8\beta_{pd}A_{2+}A_{2-}\frac{\partial \beta_{pd}}{\partial d}], \quad (112)$$

$$\frac{\partial G_{pdd2}}{\partial d} = -\frac{1}{2}\beta_{pd}\frac{\partial \beta_{pd}}{\partial d} + (2\beta_{pd}+2\beta_{pd}^3-\frac{3}{4}\beta_{pd}^5)\frac{\partial \beta_{pd}}{\partial d}(A_{2+}+A_{2-}) + 12\beta_{pd}^5 A_{2+}A_{2-}\frac{\partial \beta_{pd}}{\partial d}. \quad (113)$$

ACKNOWLEDGMENT

The authors would like to thank the National Science Council of the Republic of China (ROC) for the financial support of this research under the contract of NSC 102-2221-E-155-019.

REFERENCES

[1] R. Ulrich, "Far-infrared properties of metallic mesh and its complementary structure," *Infrared Phys.*, vol. 7, no. 1, pp. 37-50, 1967.

[2] B. A. Munk, R. J. Luebbers, and R. D. Fulton, "Transmission through a 2-layer array of loaded slots," *IEEE Trans. Antennas Propag.*, vol. AP22, no. 6, pp. 804-809, Nov. 1974.

[3] F. Yang and Y. Rahmat-Samii, "Reflection phase characterizations of the EBG ground plane for low profile wire antenna applications," *IEEE Trans. Antennas Propag.*, vol. 51, no. 10, pp. 2691-2703, Oct. 2003.

[4] Y. Zhang, J. von Hagen, M. Younis, C. Fischer, and W. Wiesbeck, "Planar artificial magnetic conductors and patch antennas," *IEEE Trans. Antennas Propag.*, vol. 51, no. 10, pp. 2704-2712, Oct. 2003.

[5] X. L. Bao, G. Ruvio, M. J. Ammann, and M. John, "A novel GPS patch antenna on a fractal hi-impedance surface substrate," *IEEE Antennas Wireless Propag. Lett.*, vol. 5, pp. 323-326, 2006.

[6] H. Mosallaei and K. Sarabandi, "Antenna miniaturization and bandwidth enhancement using a reactive impedance substrate," *IEEE Trans. Antennas Propag.*, vol. 52, no. 9, pp. 2403-2414, Sep. 2004.

[7] R. F. J. Broas, D. F. Sievenpiper, and E. Yablonovitch, "A high-impedance ground plane applied to a cellphone handset geometry," *IEEE Trans. Microw. Theory Tech.*, vol. 49, no. 7, pp. 1262-1265, Jul. 2001.

[8] A. P. Feresidis, G. Goussetis, S. Wang, and J. C. Vardaxoglou, "Artificial magnetic conductor surfaces and their application to low-profile high-gain planar antennas," *IEEE Trans. Antennas Propag.*, vol. 53, no. 1, pp. 209-215, Jan. 2005.

[9] H. Y. Chen and Y. Tao, "Bandwidth enhancement

of a U-slot patch antenna using dual-band frequency selective surface with double rectangular ring elements," *Microw. Opt. Technol. Lett.*, vol. 53, no. 7, pp. 1547-1553, Jul. 2011.

[10] H. Y. Chen and Y. Tao, "Performance improvement of a U-slot patch antenna using a dual-band frequency selective surface with modified Jerusalem cross elements," *IEEE Trans. Antennas Propag.*, vol. 59, no. 9, pp. 3482-3486, Sep. 2011.

[11] M. Philippakis, C. Martel, D. Kemp, M. C. S. M. R. Allan, S. Appleton, W. Damerell, C. Burton, and E. A. Parker, *Application of FSS Structures to Selectively Control the Propagation of Signals into and out of Buildings*, ERA Technology, Leatherhead, Surrey, UK, Tech. Rep., 2004.

[12] M. Gustafsson, A. Karlsson, A. P. P. Rebelo, and B. Widenberg, "Design of frequency selective windows for improved indoor outdoor communication," *IEEE Trans. Antennas Propag.*, vol. 54, no. 6, pp. 1897-1900, Jun. 2006.

[13] G. I. Kiani, L. G. Osslon, A. Karlsson, and K. P. Esselle, "Transmission of infrared and visible wavelengths through energy-saving glass due to etching of frequency-selective surfaces," *IET Microw. Antennas Propag.*, vol. 4, pp. 955-961, 2010.

[14] G. I. Kiani, L. G. Osslon, A. Karlsson, K. P. Esselle, and M. Nilsson, "Cross-dipole bandpass frequency selective surface for energy-saving glass used in building," *IEEE Trans. Antennas Propag.*, vol. 59, no. 2, pp. 520-525, Feb. 2011.

[15] D. J. Kern, D. H. Werner, A. Monorchio, L. Lanuzza, and M. J. Wilhelm, "The design synthesis of multiband artificial magnetic conductors using high impedance frequency selective surfaces," *IEEE Trans. Antennas Propag.*, vol. 53, no. 1, pp. 8-17, Jan. 2005.

[16] J. McVay, N. Engheta, and A. Hoorfar, "High impedance metamaterial surfaces using Hilbert-curve inclusions," *IEEE Microw. Wireless Compon. Lett.*, vol. 14, pp. 130-132, 2004.

[17] J. Bell and M. Iskander, "A low-profile archimedean spiral antenna using an EBG ground plane," *IEEE Antennas Wireless Propag. Lett.*, vol. 3, pp. 223-226, 2004.

[18] R. Mittra, C. H Chan, and T. Cwik, "Techniques for analyzing frequency selective surfaces - a review," *Pro. IEEE*, vol. 76, no. 12, pp. 1593-1615, Dec. 1988.

[19] F. R. Yang, K. P. Ma, Y. Qian, and T. Itoh, "A uniplanar compact photonic-bandgap (UC-PBG) structure and its applications for microwave circuits," *IEEE Trans. Microw. Theory Tech.*, vol. 47, no. 8, pp. 1509-1514, Aug. 1999.

[20] K. Sarabandi and N. Behdad, "A frequency selective surface with miniaturized elements," *IEEE Trans. Antennas Propag.*, vol. 55, no. 5, pp. 1239-1245, May 2007.

[21] T. Kamgaing and O. M. Ramahi, "Design and modeling of high-impedance electromagnetic surfaces for switching noise suppression in power planes," *IEEE Trans. Electromagn. Compat.*, vol. 47, no. 3, pp. 479-489, Aug. 2005.

[22] T. K. Wu, "Four-band frequency selective surface with double-square-loop patch elements," *IEEE Trans. Antennas Propag.*, vol. 42, no. 12, pp. 1659-1663, Dec. 1994.

[23] H. L. Liu, K. L. Ford, and R. J. Langley, "Design methodology for a miniaturized frequency selective surface using lumped reactive components," *IEEE Trans. Antennas Propag.*, vol. 57, no. 9, pp. 2732-2738, Sep. 2009.

[24] R. R. Xu, H. C. Zhao, Z. Y. Zong, and W. Wu, "Dual-band capacitive loaded frequency selective surfaces with close band spacing," *IEEE Microw. Wireless Compon. Lett.*, vol. 18, no. 12, Dec. 2008.

[25] G. I. Kiani, K. L. Ford, K. P. Esselle, A. R. Weily, C. Panagamuwa, and J. C. Batchelor, "Single-layer bandpass active frequency selective surface," *Microw. Opt. Technol. Lett.*, vol. 50, no. 8, pp. 2149-2151, Aug. 2008.

[26] G. I. Kiani, K. L. Ford, K. P. Esselle, A. R. Weily, and C. J. Panagamuwa, "Oblique incidence performance of a novel frequency selective surface absorber," *IEEE Trans. Antennas Propag.*, vol. 55, no. 10, pp. 2931-2934, Oct. 2007.

[27] B. A. Munk, P. Munk, and J. Pryor, "On designing Jaumann and circuit analog absorbers (CA absorbers) for oblique angle of incidence," *IEEE Trans. Antennas Propag.*, vol. 55, no. 1, pp. 186-193, Jan. 2007.

[28] A. K. Zadeh and A. Karlsson, "Capacitive circuit method for fast and efficient design of wideband radar absorbers," *IEEE Trans. Antennas Propag.*, vol. 57, no. 8, pp. 2307-2314, Aug. 2009.

[29] A. Itou, O. Hashimoto, H. Yokokawa, and K. Sumi, "A fundamental study of a thin wave absorber using FSS technology," *Electron. Commun. Jpn.*, vol. 87, pt. 1, pp. 77-86, 2004.

[30] A. Itou, H. Ebara, H. Nakajima, K. Wada, and O. Hashimoto, "An experimental study of a wave absorber using a frequency-selective surface," *Microw. Opt. Technol. Lett.*, vol. 28, pp. 321-323, 2001.

[31] G. I. Kiani, A. R. Weily, and K. P. Esselle, "A novel absorb/transmit FSS for secure indoor wireless networks with reduced multipath fading," *IEEE Microw. Wireless Compon. Lett.*, vol. 16, no. 6, pp. 378-380, 2006.

[32] N. Engheta and R. W. Ziolkowski, *Metamaterials: Physics and Engineering Explorations*, Hoboken/Piscataway, NJ, Wiley-IEEE Press, 2006.
[33] R. Baggen, M. Martinez-Vazquez, J. Leiss, and S. Holzwarth, "Comparison of EBG substrates with and without vias for GALILEO/GPS applications," In *Proc. EuCAP 2007, 2nd European Conf. Antennas Propag.*, Edinburgh, UK, 2007.
[34] Y. Fan, B. L. Ooi, H. D. Hriston, and M. S. Leong, "Compound diffractive lens consisting of Fresnel zone plate and frequency selective screen," *IEEE Trans. Antennas Propag.*, vol. 58, no. 6, pp. 1842-1847, Jun. 2010.
[35] P. Harms, R. Mittra, and W. Ko, "Implementation of the periodic boundary-condition in the finite-difference time-domain algorithm for FSS structures," *IEEE Trans. Antennas Propag.*, vol. 42, no. 9, pp. 1317-1324, Sep. 1994.
[36] J. L. Volakis, T. Ozdemir, and J. gong, "Hybrid finite-element methodologies for antennas and scattering," *IEEE Trans. Antennas Propag.*, vol. 45, no. 3, pp. 493-507, Mar. 1997.
[37] T. W. Leonard and J. W. Cofer, "A new equivalent circuit representation for the Jerusalem cross," in *Proc. IEE Int. Conf. Antennas and Propagation*, London, England, vol. 2, pp. 65-69, 1978.
[38] R. J. Langley and A. J. Drinkwater, "Improved empirical model for the Jersalem cross," *IEE Proc.*, vol. 129, Pt. H., no. 1, pp. 1-6, Feb. 1982.
[39] M. Hosseinipanah and Q Wu, "Equivalent circuit model for designing of Jerusalem cross-based artificial magnetic conductors," *Radioeng.*, vol. 18, no. 4, pp. 544-550, Dec. 2009.
[40] L. H. Lafara, *Computer Method for Science and Engineering*, New York: Hayden, pp. 148-157, 1973.
[41] S. H. Sun and B. Z. Wang, "Parameter optimization based on GA and HFSS," *J. Electron. Sci. Technol. China*, vol. 3, no. 1, pp. 45-47, Mar. 2005.

Hsing-Yi Chen was born in Taiwan, in 1954. He received the B.S. and M.S. degrees in Electrical Engineering in 1978 and 1981 from Chung Yuan Christian University and National Tsing Hua University, respectively. He received the Ph.D. degree in Electrical Engineering from University of Utah, Salt Lake City, Utah in 1989. He joined the faculty of the Department of Electrical Engineering, Yuan Ze University, Taiwan, in September 1989. He was the Chairman of Electrical Engineering from 1996 to 2002, the Chairman of Communications Engineering from 2001 to 2002, the Dean of Engineering College from 2002 to 2006, the Dean of Electrical and Communication Engineering College from 2006 to 2012, and the Dean of Research and Development Office from 2012 to 2013. Currently, he is the Dean of General Affairs Office, Yuan Ze University. His current interests include electrostatic discharge, electromagnetic scattering and absorption, waveguide design, radar systems, electromagnetic compatibility and interference, bioelectromagnetics, electromagnetic radiation hazard protection, and applications of frequency selective surface.

He is a Member of Phi Tau Phi. He was also a Member of the editorial board of the *Journal of Occupational Safety and Health* from 1996 to 1997. He was elected an Outstanding Alumnus of the Tainan Second High School in 1995. He has been the recipient of numerous awards including the 1990 Distinguished Research, Service, and Teaching Award presented by the Yuan Ze University, the 1999 and 2002 YZU Outstanding Research Award, and the 2005 Y. Z. Hsu Outstanding Professor Award for Science, Technology & Humanity Category. He was awarded Chair Professor by Far Eastern Y. Z. Hsu Science and Technology Memorial Foundation in 2008. His name is listed in Who's Who in the World in 1998.

Tsung-Han Lin was born in Taiwan, in 1988. He received the B.S. degree in Electronic Engineering from Chung Yuan Christian University in 2010. He is currently working toward the M.S. degree in Communications Engineering at Yuan Ze University, Taiwan. His research interests include patch antenna design, frequency selective surfaces, and numerical computation of electromagnetics.

Pei-Kuen Li was born in Taiwan, in 1988. He received the B.S. and M.S. degrees in Communications Engineering from Yuan Ze University in 2011 and 2013, respectively. His research interests include electrostatic discharge, patch antenna design, electromagnetic compatibility and interference, wireless communications, and numerical computation of electromagnetics.